# Fiber Bragg Grating Sensor for Strain Sensing in Low Temperature Superconducting Magnet

Hongjie Zhang, Qiuliang Wang, Housheng Wang, Shousen Song, Baozhi Zhao, Yinming Dai, Guojun Huang, and Zhonghua Jiang

***Abstract*—Fiber Bragg grating (FBG) sensor for monitoring the electromagnetic strain in a low temperature superconducting (LTS) magnet was studied. Before used to LTS magnet strain sensing, the strain response of the sensor with 1.54-$\mu$m wavelength at liquid helium was experimentally studied. It was found that the wavelength shift showed good linearity with longitudinal applied loads and the strain sensitivity is constant at 4.2 K. And then, the hoop strain measurement of a LTS magnet was carried out on the basis of measured results. Furthermore, the finite element method (FEM) was used to simulate the magnet strain. The difference between the experimental and numerical analysis results is very small.**

***Index Terms*—Fiber Bragg grating, liquid helium temperature, LTS magnet, strain sensing.**

## I. Introduction

THE tendency of coils to quench prematurely, at relatively low fractions of the critical current, or to exhibit training behavior, is often attributed to mechanical issues. A knowledge of stress, strain, and displacement of the windings, is therefore central to the design of the superconducting magnet [1]. The resistive foil strain gauge (RFSG) has remained the device most commonly used for measuring the strain on cryogenic structures. The nonlinear thermal apparent strains and measurement sensitivity to electromagnetic noise remain the most significant limitations to its successful implementation [2], [3]. Fiber Bragg grating (FBG) sensor has a number of distinct advantages over other sensors, such as electromagnetic interference (EMI) immunity, high sensitivity, and compact size. Furthermore, the wavelength-encoded nature allows the distributed sensing of strain [4]–[6]. Fiber Bragg gratings (FBGs) are used to monitor temperature and strain in engineering structures; to date, however, their use has been limited to ambient and high temperatures, typically in the range of 273 K to 773 K.

Manuscript received October 18, 2009. First published April 05, 2010; current version published May 28, 2010. This work was supported by the National Natural Science Foundation of China 50925726 and 50577063.

H. Zhang is with Key Laboratory of Applied Superconductivity, Institute of Electrical Engineering, Chinese Academy of Sciences (IEE, CAS), Beijing, China (e-mail: hjzh@mail.iee.ac.cn).

Q. Wang, H. Wang, S. Song, B. Zhao, and Y. Dai are with Applied Superconductor Laboratory, IEE, CAS, Beijing, China.

G. Huang and Z. Jiang are with Institute of Mechanics, Chinese Academy of Sciences, Beijing, China.

Color versions of one or more of the figures in this paper are available online at http://ieeexplore.ieee.org.

Digital Object Identifier 10.1109/TASC.2010.2042693

FBG sensor used to strain sensing at 77 K and used in high temperature superconducting (HTS) magnet has been reported [7]. To date, FBG sensor used to strain sensing at 4.2 K and used in low temperature superconducting (LTS) magnet has not been reported yet. Before used to monitor the strain in LTS magnet, the strain characteristics of FBG at liquid helium temperature were experimentally studied. Basing on the results, the FBG sensor was used in LTS magnet for strain sensing for initial attempt.

## II. Strain Sensing Theory of FBG Sensor

An FBG is a periodic modulation of the index of refraction in the core of an optical fiber formed by exposure to UV radiation. The Bragg reflection wavelength of an FBG is given as

$$\lambda_B = 2n_{eff}\Lambda \tag{1}$$

where $n_{eff}$ is the effective refractive index of the core and $\Lambda$ is the grating period.

The FBG is sensitive to both strain and temperature. The strain response arises from both the physical elongation of the sensor and the change in fiber index because of photoelastic effects [6]. The shift in Bragg wavelength with strain can be defined as

$$\Delta\lambda_{BS} = (1 - p_e)\lambda_B \cdot \varepsilon \tag{2}$$

where $\varepsilon$ is the applied strain, and $p_e$ is an effective photoelastic coefficient. $p_e = 0.22$ at room temperature.

The strain sensitivity is expressed as

$$K_s = (1 - p_e)\lambda_B. \tag{3}$$

The dependence of the Bragg wavelength on temperature arises due to two primary effects: the dependence or the index of refraction of the glass on temperature and the thermal expansion of the glass. The thermal induced wavelength shift is defined as

$$\Delta\lambda_{BT} = \lambda_B(\alpha + \xi)\Delta T. \tag{4}$$

It has been reported that the thermal sensitivity of FBG is nonlinear [8]. Due to the refractive index of fused silica approaches zero as the temperature nears absolute zero, the thermal sensitivity decreases with low temperature, and to approximately zero at liquid helium temperature (4.2 K). We have also experimentally confirmed the result [9] which offers the prospect of temperature-insensitive strain measurement in cryogenic environments.

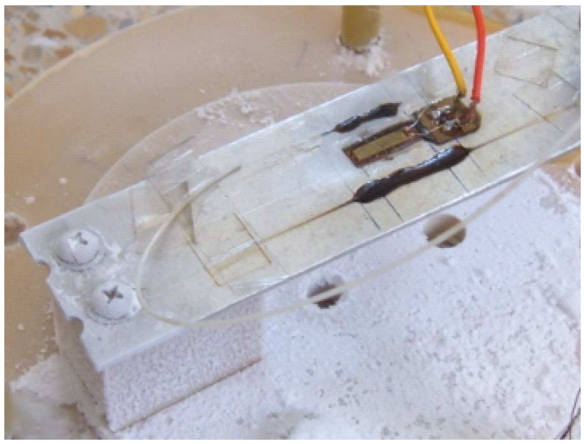

Fig. 1. Cantilever set-up for strain response measurement at 4.2 K.

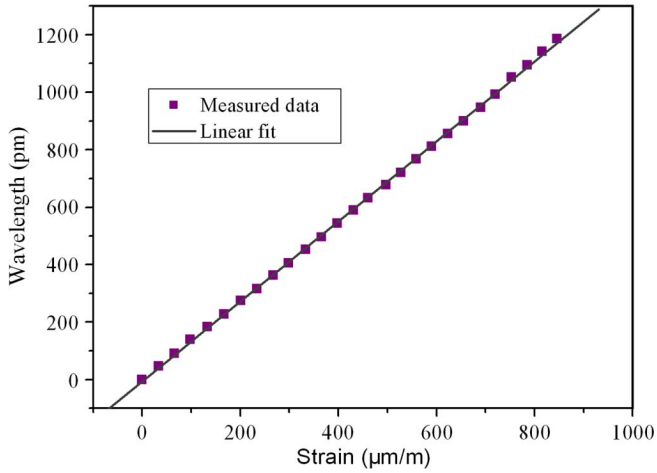


Fig. 2. Wavelength shift of the FBG sensor with strain at 4.2 K.

As discussed in (1), the FBG sensor is sensitive to both strain and temperature. This creates a problem with sensor systems designed to monitor distributed strain. In order to discriminate strain response with the temperature response, the wavelength is used as a reference wavelength at the moment current is zero in our experiment.

## III. Experimental Procedure

### A. Strain Response of FBG Sensor at 4.2 K

The section describes experiments to measure and calibrate the response of an FBG sensor to longitudinal strain. An FBG with 1.54-$\mu$m center wavelength was tested. The grating length is 15 mm, and the bandwidth is 0.3 mm. The experiments were based on the principle of cantilever, as shown in Fig. 1. The cantilever beam was made of an Aluminum fixed on one end. Its thickness is 3 mm. The FBG was attached onto the surface of cantilever with DW3 epoxy adhesive. A resistance strain gauge near the FBG was used as strain reference, which was attached with the same adhesive. And a rhodium iron thermometer was placed on the surface of cantilever freely to measure the environment temperature.

The experiments were performed within a cryostat. The cryostat was cooled down from room temperature to 4.2 K by liquid helium. After the temperature was stable, longitudinal loads were applied to the cantilever by the means of a stainless steel pole through the top plate. As a result, the cantilever was deflected and the wavelength of FBG sensor was changed. The loads were applied in step of 0.25 mm to a maximum of 6.5 mm. The reflection spectrum and the wavelength shift were examined with a portable FBG demodulation system.

### B. Strain Sensing in LTS Magnet

The described test as follows was conducted in an attempt to verify the ability of the FBG sensor to detect strain of the LTS magnet and thereby prove the general possibility to use the sensor for high magnetic field magnet monitoring at cryogenic temperature.

After the previous test, the experiment for strain sensing in a LTS magnet was carried out. In the FBG sensor strain response experiment, the wavelength of the sensor showed good linear dependence on the applied strain at 4.2 K, as shown in Fig. 2. It indicated that the FBG sensor can be used as a strain sensor at liquid helium temperature.

The LTS magnet system consists of four NbTi solenoids fabricated using rectangular wire with the dimension of 2.2 $\times$ 1.4 mm. To improve liquid helium cooling abilities, the superconducting solenoid was dry wound with narrow liquid helium channels between adjacent layers. Stainless steel was chosen as the former for magnet fabrication for its relative low thermal contraction. Totally 4 layers of stainless steel wire were tightly wound as the overbinding layer.

In the superconducting magnet structural health monitoring, the distributed or maximum strain was expected to be examined. Because the magnet is dry wound, and liquid helium channels existed between adjacent layers, it was difficult to place the FBG sensors during winding. Four FBG sensors were attached the surface of stainless steel overbinding of the LTS magnet, as shown in Fig. 3. In order to obtain the distributed strain, three FBG sensors (FBGS1 $\sim$ FBGS3) were attached along the half-height of the bottom coil, and one FBG sensor (FBGS4) was attached near the middle plate of the solenoid. Before fixing the FBG sensors, the fiber-glass tapes were wrapped outside the stainless steel binding together with epoxy resin. And then the FBG sensors were fixed in tension on the tapes circumferentially and attached by DW3 adhesive. At last, the sensors were covered by fiber-glass tapes together with epoxy resin. All the processes ensured the sensors could sense the real strain.

The experiments were performed within a cryostat. During the test, the LTS magnet was cooled down by liquid nitrogen to 77 K and liquid helium to 4.2 K. After the magnet was cooled down to 4.2 K completely, the magnet was excited from zero up to 290 A, the FBG sensors spectra and center wavelength shifts were monitored by Optical Sensing Interrogator (OSI)(sm125).

## IV. Numerical Simulation

The finite element method (FEM) was used to simulate the magnet strain. In the magnet, the four solenoids distribute uniformly along $\varnothing$0.28 m circumference. Because the magnet is


Fig. 3. Picture of FBG sensors attached on the LTS magnet.

TABLE I
MAIN PARAMETERS OF THE LTS MAGNET

| | |
|---|---|
| Superonductor | NbTi/Cu |
| Inner Diameter (mm) | 93 |
| Outer Diameter (mm) | 136 |
| Height (mm) | 571 |
| Layers of Single Coil | 26 |
| Turns of Single Coil | 3250 |
| Operating Current (A) | 290 |
| Maximum Magnetic Field (T) | 4.39 |

centrosymmetric and the magnetic forces were assumed to be uniformly distributed in the magnet, 3D 1/8th model was used. The dimensions of the solenoid are listed in Table I. Fig. 4 shows the magnetic field distribution in the magnet when the operating current is 290 A. The unit of the magnetic filed is Tesla (T). The maximum magnetic field is about 4.4 T located at the inner coil of the magnet. The minimum magnetic field is about 0.01 T, which is located at the outside coil. The hoop strain results are plotted in Fig. 5 at the same current. The unit of the strain is Micro-strain ($\mu$m/m). The maximum hoop strain is 137 $\mu$m/m (0.0137%) in the magnet and 73.5 $\mu$m/m (0.00735%) in stainless steel overbinding.

In order to produce high magnetic field in the clear bore, the operating currents in adjacent solenoids were designed to be in the opposite direction, and the currents in the opposite solenoids were in the same direction. The adjacent solenoids present at the magnetic field afforded tremendous attractive magnetic force. In order to prevent the solenoids from moving and support the magnet, the adjacent solenoids were designed to contact at the middle plate. As a result, the strain in the magnet and overbinding is very small. The calculated strain at the position where FBGS4 is attached is listed in Table II.

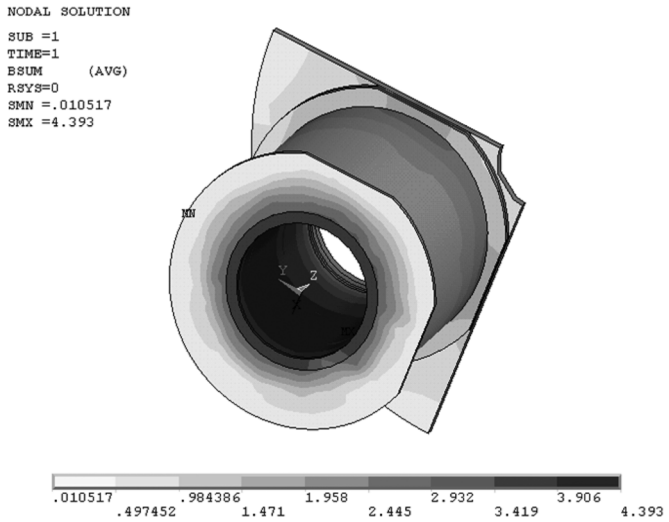


Fig. 4. Magnetic field of the tested coil. The excited current in the magnet is 290 A. The unit of the magnetic filed is T. The maximum magnetic field is about 4.4 T and the minimum is about 0.01 T.

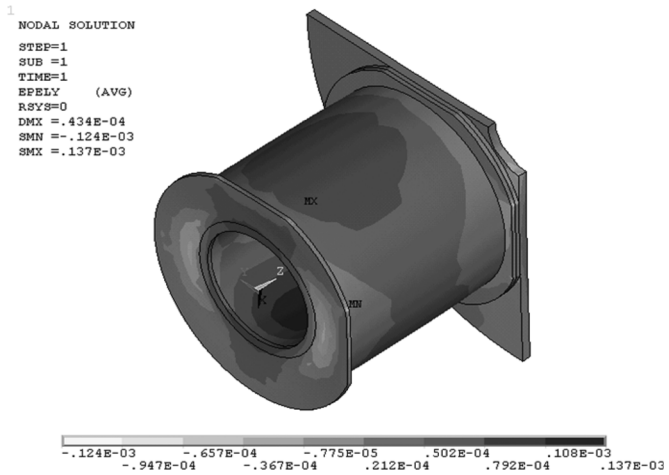


Fig. 5. Hoop strain of the tested coil. The excited current in the magnet is 290 A. The unit of the strain is Micro-strain ( ). The maximum hoop strain is 137 (0.0137%) in the magnet and 73.5 (0.00735%) in stainless steel overbinding.

TABLE II
MAXIMUM MAGNETIC FIELD AND HOOP STRAIN/STRESS OF THE TESTED COIL

| I (A) | $B_{max}$ (T) | Hoop displacement (mm) | Hoop stress (MPa) | Hoop strain (μm/m) |
|---|---|---|---|---|
| 150 | 2.31 | 0.207E-02 | 0.935 | 6.949 |
| 175 | 2.70 | 0.282E-02 | 1.273 | 9.458 |
| 200 | 3.08 | 0.369E-02 | 1.662 | 12.353 |
| 225 | 3.47 | 0.467E-02 | 2.104 | 15.635 |
| 250 | 3.85 | 0.577E-02 | 2.597 | 19.302 |
| 275 | 4.24 | 0.698E-02 | 3.143 | 23.355 |
| 290 | 4.39 | 0.777E-02 | 3.499 | 25.994 |

## V. Results and Discussion

Fig. 2 shows the wavelength shift of the FBG sensor with strain at 4.2 K. The wavelength shift observed for the FBG senor was dominated by the strain induced by the deflection of cantilever, and did not consider the temperature-induced wavelength shift. It was found that the wavelength of FBG sensor depends linear on applied strain at 4.2 K. The measured strain sensitivity of the 1.54-$\mu$m FBG sensor is 1.4 $\mathrm{pm}(\mu\mathrm{m/m})^{-1}$. It is larger than the theoretical value of 1.201 $\mathrm{pm}(\mu\mathrm{m/m})^{-1}$ referring to (3) at room temperature. FBG strain response was measured in the range temperature from 2.2 K to 280 K, and the strain sensitivity was found to be independent of temperature by James *et al.* [10]. In [11] strain response of FBG sensors were measured over a temperature range of 123 K to 317 K, and the strain sensitivity was found to be temperature-dependent, increasing with decreasing temperature. The authors of [11] also analysed that lower resolution of measurement brought the different results. The strain response measurement was repeated three times in our experiment, and the consistent response results were obtained. Therefore, the FBG sensor and strain sensitivity were used in the LTS magnet strain measurement.

In the magnet experiment, four FBG sensors were used to measure magnet strain. As the magnet was cooled down, the wavelength of all sensors decreased with the temperature. When the temperature descended to 4.2 K, the spectra of the sensors along the half-height of the bottom coil split. The peaks probably come from the non-uniform strain. To reduce the strain produced by electromagnetic force, the solenoid was separated by middle plate. The strain at the half-height of the bottom coil is much higher than that near the end of middle plate. The higher strain made the stainless steel wire move, and the DW3 adhesive on the sensors cracked. As a result, the sensors at the middle of the coil suffered non-uniform strain. The wavelength of FBGS4 shifted with temperature and had a single peak at liquid helium temperature. The experimental hoop strain at operating currents is compared with the numerical results and plotted in the Fig. 6. The difference between them is small. When the magnet was excited from zero up to 290 A, the magnetic filed in the magnet increased with current, and the strain caused by the magnetic field increased also. In the initial stage, the electromagnetic strain of the magnet was small, so the calculated data is larger than the measured data. With the increase of the excited current, the measured results are close to the numerical results. The difference between them is probably caused by disturbance of the power supply.

## VI. Conclusion

We have found experimentally that the wavelength of FBG sensor depends linear on applied strain at 4.2 K. The strain sensitivity of the 1.54-$\mu$m FBG is 1.4 $\mathrm{pm}(\mu\mathrm{m/m})^{-1}$ at liquid helium. According to the results, the FBG sensors were used to measure the hoop strain in the LTS magnet, the measured value is close to the theoretical analysis.

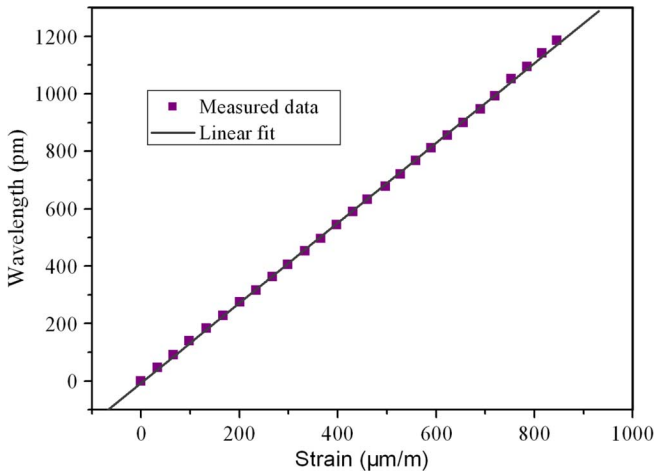


Fig. 6. Tested results verse simulation results.

Further experiments will use the FBG sensor at high magnetic field for high strain measurement and attempt to mount the sensor inside the magnet during winding. Distributed and real time strain measurement will be realized.

## Acknowledgment

The authors would like to thank H. Liu, J. cheng, and S. Chen for their assistance in the experiment. They would also like to thank the instruments and technical support of Micron Optics International Beijing Representative.

## References

[1] M. R. Vaghar, H. Garmestani, and W. D. Markiewicz, "Elastoplastic stress analysis of Nb3Sn superconducting magnet," *J. Appl. Phys.*, vol. 80, no. 4, pp. 2490–2500, 1996.

[2] J. C. Telinde, "Strain gages in cryogenic environment," *Experimental Mechanics*, vol. 10, no. 6, pp. 394–400, 1970.

[3] P. L. Walstrom, "The effect of high magnetic fields on metal foil strain gauges at 4.2 K," *Cryogenics*, vol. 15, no. 5, pp. 270–272, 1975.

[4] A. D. Kersey, M. A. Davis, H. J. Patrick, M. LeBlane, K. P. Kao, C. G. Atkins, M. A. Putnam, and E. J. Friebele, "Fiber grating sensors," *J. Lightwave Technol.*, vol. 15, no. 8, pp. 1442–1462, 1997.

[5] K. O. Hill and G. Meltz, "Fiber Bragg grating technology fundamentals and overview," *J. Lightwave Technol.*, vol. 15, pp. 1263–1275, 1997.

[6] A. D. Kersey, "A review of recent developments in fiber optic sensor technology," *Optic. Fiber Technol.*, vol. 2, pp. 291–317, 1996.

[7] Q. Wang, Z. Feng, F. Deng, G. Huang, L. Yan, and Y. Dai, "Fiber Bragg gratings for strain sensing in high temperature superconducting magnet," *IEEE Trans. Appl. Supeconduct.*, vol. 17, no. 2, pp. 2377–2380, June 2007.

[8] M. B. Reld and M. Ozcan, "Temperature dependence of fiber optic Bragg gratings at low temperatures," *J. Opt. Eng.*, vol. 37, no. 1, pp. 237–240, 1998.

[9] H. J. Zhang, F. P. Deng, Q. L. Wang, L. G. Yan, Y. M. Dai, and K. Kim, "Development of strain measurement in superconducting magnet through fiber Bragg grating," *IEEE Trans. Appl. Supeconduct.*, vol. 18, no. 2, pp. 1419–1422, 2008.

[10] S. W. James, R. P. Tatam, A. Twin, M. Morgan, and P. Noonan, "Strain response of fibre Bragg grating sensors at cryogenic temperatures," *Meas. Sci. Technol.*, vol. 13, pp. 1535–1539, 2002.

[11] X. Zhang, Z. Wu, and B. Zhang, "Strain dependence of fiber Bragg grating sensors at low temperature," *Optical Engineering*, vol. 45, no. 5, pp. 054401-1–054401-4, 2006.